Chemistry and Materials

The Center for Science Innovation

Research Article

Chem. Mater. 3 (1) 2024, 27-33

The Effect of Electrodeposition Voltage on the Antioxidant Activity of Gold Nanoparticles

Babay Asih Suliasih[1*], Anis Sakinah[2], Marissa Angelina[3]

[1]Faculty of Pharmacy, Universitas Indonesia, Gedung A Rumpun Ilmu Kesehatan, Kampus UI Depok, Pondok Cina, Kecamatan Beji, Kota Depok, Jawa Barat, 16424, Indonesia

[2]Department of Chemistry, Faculty of Mathematics and Science, Universitas Negeri Jakarta, Jl. Rawamangun Muka, Jakarta 13220, Indonesia

[3]Indonesia Research Centre for Pharmaceutical Ingredients and Traditional Medicine, National Research and Innovation Agency (BRIN), Kawasan PUSPIPTEK Serpong, Tangerang Selatan Banten 15314, Indonesia

*Corresponding author: babay_asih@farmasi.ui.ac.id

Received
8 January 2024

Received in revised form
16 February 2024

Accepted
23 February 2024

Published online
29 February 2024

DOI
https://doi.org/10.56425/cma.v3i1.72

Abstract

Gold nanoparticles (AuNPs) are well known as free radical scavengers, which may induce cell damage, triggering degenerative diseases and premature aging. This research aims to assess the antioxidant activity of AuNPs synthesized via the electrodeposition method, employing cyclic voltammetry on a Fluorine-doped Tin Oxide (FTO) substrate. By varying the initial voltage, the resulting AuNPs exhibit variations in both particle size and number. In this study, AuNPs demonstrated promising antioxidant potential, particularly at an initial voltage of -1 V, as evidenced by their ability to respond to DPPH radicals, yielding a percent inhibition of up to 36.80%.

Keywords: antioxidants, electrodeposition, gold nanoparticles.

1. Introduction

Antioxidants are compounds capable of delaying, controlling, or inhibiting the autooxidation process [1]. Antioxidants are compounds that function as cellular defenders against the harmful effects of free radicals. By donating electrons to neutralize the unpaired electrons of free radicals, antioxidants disrupt the chain reaction of free radical formation, thereby mitigating the oxidative stress that leads to cellular damage [2].

The effectiveness of natural antioxidants and certain synthetic antioxidants is constrained by factors such as poor absorption, limited ability to traverse cell membranes, and susceptibility to degradation during transportation. The advancements in nanotechnology have facilitated the utilization of nanoparticles derived from inorganic materials as novel antioxidants exhibiting enhanced properties [3].

Gold nanoparticles (AuNPs) are among the numerous nanomaterials known for their potential as antioxidants. These nanoparticles are recognized for their ability to scavange free radicals, which are implicated in cellular damage, leading to the onset of degenerative diseases and premature aging [4]. Numerous studies have demonstrated that the kinetic activity of radical scavenging, both in vivo and in vitro, indicated that AuNPs serve as potent antioxidants, exhibiting a notable capacity for scavenging reactive oxygen species (ROS) in living cells [3]. When compared with natural antioxidants, synthetic antioxidants made from AuNPs exhibit three times more effective antioxidant activity [5] and do not have carcinogenic effects in the body [4].

The AuNPs are commonly employed as support agents for various applications, and they are typically synthesized using biosynthesis methods [6-10]. Nevertheless, this approach necessitates considerable energy consumption and high cost [11]. In addition, the synthesis of AuNPs using the colloidal phase biosynthesis method involves a phase that cannot solely account for AuNPs as an antioxidant; instead, it is also influenced by other compounds [12- 16].

One of the most attractive alternative methods is the electrodeposition method. This method has been proven by many researchers to be capable of synthesizing AuNPs, resulting in the deposition of AuNPs onto the substrate surface to form a thin film [17–21]. The method provides several advantages, including simplicity, speed, and cost-effectiveness. Furthermore, it offers the ability to control the particle size, crystallographic orientation, mass, thickness, and morphology of the nanostructured materials by adjusting the operating conditions and bath chemistry [22]. The utilization of cyclic voltammetry is frequently observed in the process of electrodeposition synthesis to produce nanomaterials. Cyclic voltammetry allows for control over the deposition process by adjusting the potential within a range of values [23].

Therefore, this research aims to determine the response of antioxidant activity to AuNPs, which serve as the primary antioxidants. These antioxidants are synthesized using the electrodeposition method with cyclic voltammetry techniques, resulting in AuNPs with either a solid or thin film phase. This synthesis process avoids the use of additives containing antioxidant compounds. Consequently, the study aims to observe the mechanism of AuNPs acting as single antioxidants.

2. Materials and Method

The materials used in this research are $HAuCl_4.3H_2O$, H_2SO_4, DPPH (2,2-diphenyl-1-picrylhydrazyl) and Fluorine-doped Tin Oxide glass as a substrate.

The AuNPs synthesis process was conducted using 15 mL of 0.5 mM $HAuCl_4 \cdot 3H_2O$ in 0.5 M H_2SO_4 as an electrolyte solution, employing a cyclic voltammetry technique with a scan rate of 100 mV/s, 50 cycles, a final voltage of 1.5 V, and varying the initial voltage. The initial voltage variations used were as follows: -0.25 V, -0.4 V, -0.75 V, -1 V, and -1.5 V. AuNPs were synthesized on an FTO substrate, which functioned as the working electrode, while the platinum plate served as the counter electrode, and Ag/AgCl was the reference electrode. All treatments were conducted at room temperature (25°C). After the electrodeposition process was completed, the AuNPs deposited on the FTO substrate were removed from the cell, rinsed with distilled water, and dried.

The obtained AuNPs were subsequently subjected to characterization using an energy-dispersive X-ray spectrometer (EDX, Qxford Instrument: Xplore 15) and a Scanning Electron Microscope (SEM) (Thermoscientific: Quanta 650) to analyze their elemental composition and morphology. Concurrently, the determination of particle size was carried out utilizing ImageJ software. In addition, the characterization of the AuNPs structure involved the use of X-ray Diffraction (XRD) (Panalytical AERIS) analysis, to investigate the crystalline nature of the nanoparticles.

The DPPH assay was employed to assess the antioxidant activity of AuNPs, with measurements taken using a Microplate Reader Spectrophotometer (Thermo Scientific: Elisa Reader). The AuNPs, measuring 5 mm x 15 mm, were positioned in microplate-24 wells and then immersed in 1.3 ml of 100 µM DPPH solution dissolved in ethanol. Subsequently, the specimen was shaken and incubated in a spectrophotometric instrument with various incubation times ranging from 15 to 150 minutes. Absorbance readings were taken every 15 minutes. Following this, experimentation was conducted by scanning wavelengths in the range of 300 to 750 nm.

The determination of DPPH inhibition percentage was carried out according to equation (1)

$$\% \text{ Inhibition of DPPH} = [(C–S/C)] \times 100\% \quad (1)$$

Where C is the absorbance of the DPPH control and S is the absorbance of the DPPH-AuNFs solution at 516 nm.

3. Results and Discussion

3.1. AuNPs Characterization

3.1.1. XRD

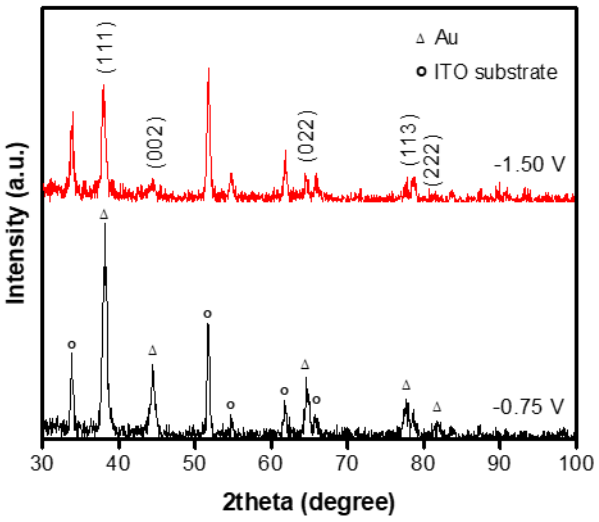

Figure 1. XRD diffraction patterns of AuNPs

The XRD characterization utilized a Cu-K-Alpha1 radiation source (λ = 1.540598 Å), operating at a potential of 40 kV and a current of 15 mA. The AuNP/FTO samples underwent scanning from 5° to 100° (2θ). Based on the XRD data acquired (Figure 1), Au crystals were identified through diffraction peaks at 2θ values of 38.24, 44.45, 64.68, 77.69, and 81.86. According to the Crystal Open Database COD No. 96-901-1614, these peaks correspond

to reflection planes (111), (002), (022), (113), and (222), respectively, from face-centered cubic Au crystal. Additionally, there is a diffraction peak attributed to the indium tin oxide (ITO) substrate.

3.1.2. EDX & SEM

The EDX result confirmed the presence of gold nanoparticles on the surface of the FTO substrate. Figure 2 illustrates the spectrum of gold nanoparticles (AuNPs), revealing signals within the energy range of 2.1 and 8.5 – 11. keV. In addition, the spectrum indicated the presence of other elements originating from the FTO substrate, specifically tin (Sn) and silicon (Si).

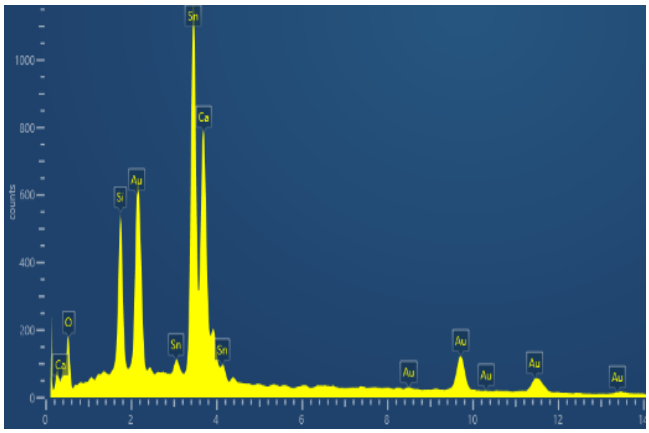

Figure 2. EDX spectrum of AuNPs

The SEM results of AuNPs deposited under different voltages are depicted in Figure 3, along with a histogram that illustrates the distribution of particles per unit area. Furthermore, the analysis of the relationship between potential with particle size and particle number is presented in Table 1. The AuNPs deposited at an initial voltage of -1 V produce evenly distributed particles with an average size of 60.95 nm. The dominant shape is spherical, with some particles appearing to overlap, and a high density between the particles. The total number of particles produced is 100,496,943/mm².

Subsequently, upon decreasing the voltage to -0.75 V, the particles exhibited an increase in size to an average of 92.22 nm, displaying a spherical shape, and the particle density was measured at 51,000,266/mm2. Further reduction of the voltage to -0.4 V results in uneven particle distribution, increased in size with an average size of 185.39 nm, an irregular or flower-like shape, and a low density between the particles. The number of particles decreases to 4,947,550/mm².

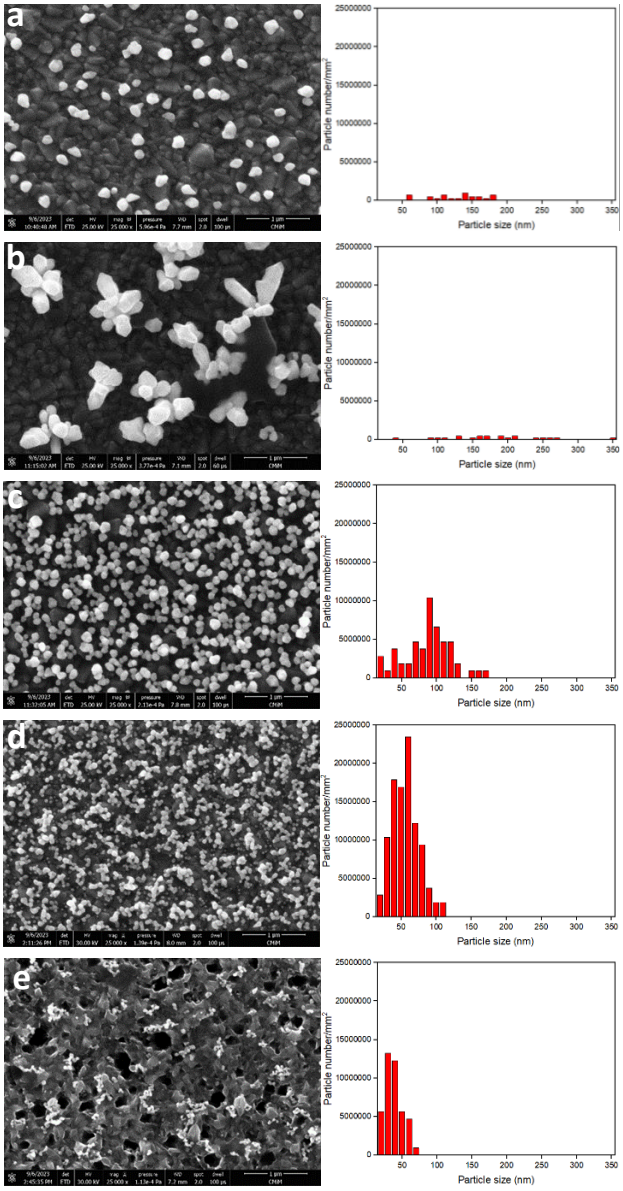

Figure 3. SEM analysis of AuNPs deposited and histogram of particle distribution per unit area at various lower potential (a) -0,25 V, (b) -0,4 V, (c) -0,75 V, (d) -1 V, and (e) -1,5 V

Continuing the voltage reduction to -0.25 V, smaller particles were generated, with an average size of 132. 79 nm and irregular morphology, accompanied by a notably low interparticle density. The number of particles produced is relatively small, totaling 5,432,759/mm².

Decreasing the initial voltage to -0. 25 V has the dual effect of narrowing the voltage range and reducing the particle deposition time. It is hypothesized that the restriction on particle growth leads to a decrease in the overlap of nuclei [24]. As a result, the particles demonstrate minimal overlap, preventing the formation of larger particles through particle fusion. This phenomenon

leads to a decrease in the number of particles as they fail to unite and retain their distinct individual entities.

Table 1 The relationship between potential with particle size and particle number.

Sample	Particle size (nm)	Particle number/mm²
-0,25 V	132,79	5.432.759
-0,4 V	185,39	4.947.550
-0,75 V	92,22	51.000.266
-1 V	60,95	100.496.943
-1,5 V	43,83	42.533.926

Nevertheless, an increase in voltage from -1 V to -1.5V led to a non-uniform distribution of particles with an average size of 43. 83 nm and irregular shapes. The particles tended to aggregate, forming islands with a relatively high density between them. Furthermore, the total number of particles produced was 42,533,926/mm². Raising the initial voltage to -1. 5 V impairs the rate of nucleation of Au and restricts its formation to localized regions on the FTO substrate, thereby yielding a limited quantity of particles. It can be inferred that the application of an initial voltage of up to -1. 5 V is suboptimal for achieving the desired level of nucleation on the surface of the FTO substrate. However, it appears adequate to provide the particles with sufficient time to undergo growth and aggregation processes [24].

3.2 Antioxidant Activity Test

As depicted in Table 2 below, the sample manifesting a voltage variation below -1 V exhibits the highest inhibition value, notably 36.80%. This observation implies that the synthesized AuNPs possess remarkable antioxidant capabilities. This phenomenon arises from the ability of AuNPs to transfer electrons to DPPH free radicals, resulting in the reduction of DPPH to a stable non-radical compound [25].

Table 2 The relationship between potential and percent inhibition in the DPPH method after 150 minutes of incubation.

Sample	Inhibition (%)
-0,25 V	15,02
-0,4 V	26,73
-0,75 V	26,87
-1 V	36,80
-1,5 V	28,06

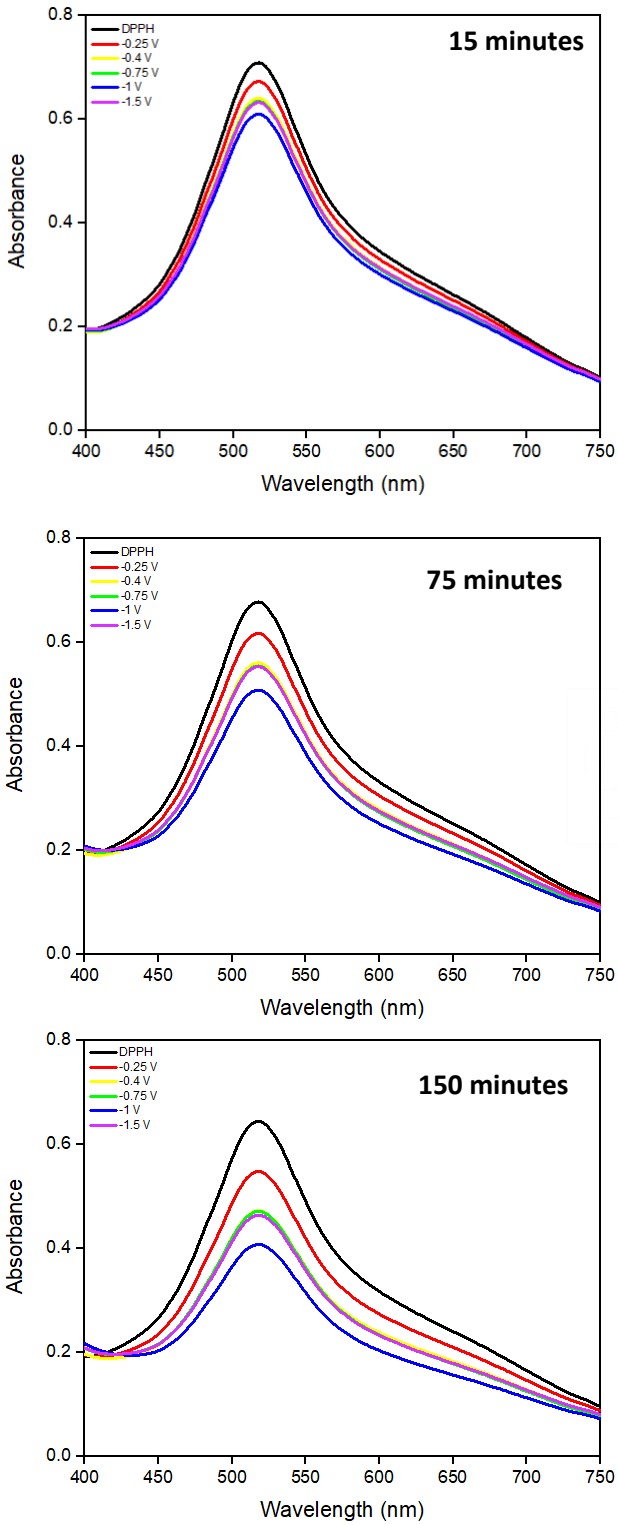

Figure 4 displays a reduction in the DPPH absorbance value for each sample of AuNPs. This study demonstrates the DPPH inhibitory activity of AuNPs, which can subsequently be quantified as a percentage inhibition to determine the optimal antioxidant power of the AuNPs.

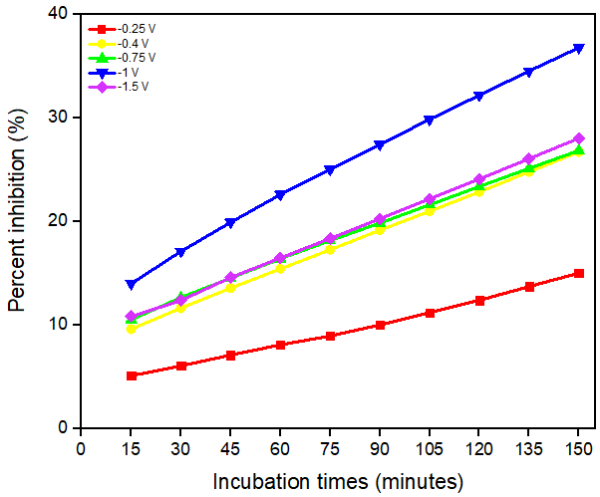

Figure 5. Spectrum UV–vis spectra of DPPH control and AuNPs samples tested after incubation 15, 75, and 150 minutes, also The inhibition percent of AuNPs synthesized at different lower potentials.

The scavenging mechanism involves AuNPs transferring their electrons and stabilizing the nitrogen atom present in DPPH through mutual binding [6]. Moreover, the formed bond is a coordinated covalent bond between gold (Au) and nitrogen (N), resulting in the quenching of the radical nature of the DPPH compound, as the N atom is stabilized by the Au atom in this state [26]. The following is a presumed mechanism for reducing DPPH free radicals by AuNPs:

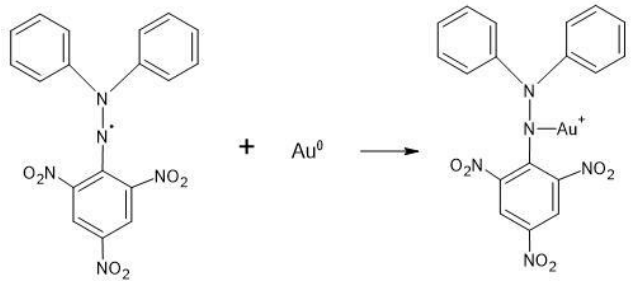

Figure 6. Mechanism of reducing DPPH free radicals by AuNPs

The process of scavenging DPPH free radicals is characterized by a color change from purple to yellow, indicating the transformation of DPPH free radicals into a more stable compound [6].

By the SEM results, the sample subjected to an initial voltage of -1 V demonstrates the most substantial percentage of inhibition, attributed to its small particle size and highest particle count compared to other samples. Moreover, the sample exhibits uniform particle distribution and relatively high density. At a voltage of -1.5 V, the produced particles are even smaller. Still, the number of particles distributed is very minimal and uneven, resulting in a decrease in the percentage of inhibition. Subsequently, as the voltage is reduced to -0.25 V, the produced inhibition percentage also decreases. This is attributed to the larger size of the particles generated and the reduced particle count. This result indicates a positive correlation between the reduction in particle size of AuNPs and the enhancement of antioxidant activity. This reduction results in an increased surface area, which in turn promotes an enhanced interaction between AuNPs and radicals. This leads to a high antioxidant activity [27].

By the SEM results, the sample subjected to an initial voltage of -1 V demonstrates the most substantial percentage of inhibition, attributed to its small particle size and highest particle count compared to other samples. Moreover, the sample exhibits uniform particle distribution and relatively high density. At a voltage of -1.5 V, the produced particles are even smaller. Still, the number of particles distributed is very minimal and uneven, resulting in a decrease in the percentage of inhibition. Subsequently, as the voltage is reduced to -0.25 V, the produced inhibition percentage also decreases. This is attributed to the larger size of the particles generated and the reduced particle count. This result indicates a positive correlation between the reduction in particle size of AuNPs and the enhancement of antioxidant activity. This reduction results in an increased surface area, which in turn promotes an enhanced interaction between AuNPs and radicals. This leads to a high antioxidant activity [27].

Moreover, the number of particles is directly proportional to the percent inhibition, indicating that a higher production of AuNPs particles leads to increased scavenging of radical species, thereby enhancing their antioxidant activity. Additionally, it was observed that longer incubation times resulted in a higher percent inhibition. This phenomenon can be attributed to the extended interaction between the AuNPs and radicals, allowing more gold particles to effectively quench the radicals [28].

4. Conclusion

Gold nanoparticles (AuNPs) synthesized through electrodeposition at varying voltages demonstrated promising potential as antioxidants, as evidenced by their ability to quench DPPH radicals. The DPPH test findings indicate that the synthesis of small-sized AuNPs with a high particle count at a voltage of -1 V effectively inhibits DPPH radicals, reaching up to 36.80%.

Acknowledgment

The authors thankfully acknowledge the support of the Institute for Research and Community Service of Universitas Negeri Jakarta (LPPM UNJ), Indonesia in the form of a research grant from International Collaborative Scheme (KI) No 24/KI/LPPM/III/2023.

References

[1] S.F. Annisa, Z. Darwis, T. Hadinugrahaningsih, The Effect of Tertiary Butylhydroquinone Antioxidant on The Stability of Rubber Seed Biodiesel, *Chem. Mater.* **1** (2022) 34–39. https://doi.org/https://doi.org/10.56425/cma.v1i2.26.

[2] R.R. Tiastika, Uji Aktivitas Penangkap Radikal Bebas dan Penetapan Kadar Fenolik Total Ekstrak Etanol Tiga Rimpang Genus Curcuma dan Rimpang Temu Kunci (boesenbergia pandurata), Universitas Muhammadiyah, 2011.

[3] I. Khalil, W.A. Yehye, A.E. Etxeberria, A.A. Alhadi, S.M. Dezfooli, N.B.M. Julkapli, W.J. Basirun, A. Seyfoddin, Nanoantioxidants: Recent trends in antioxidant delivery applications, *Antioxidants*. **9** (2020). https://doi.org/10.3390/antiox9010024.

[4] R.. Sekarsari, Taufikurrohmah, Sintesis dan Karakterisasi Nanogold dengan Variasi Konsentrasi HAuCl4 sebagai Material Antiaging dalam Kosmetik, in: Pros. Semin. Nas. Kim. Unesa 2012- ISBN 978-979-028-550-7, 2012.

[5] M.A. Amiruddin, T. Taufikurrohmah, Synthesis and Characterization of Gold Nanoparticle Using a Matrix of Bentonite in Scavenging Free Radicals in Cosmetics, *UNESA J. Chem. Vol. 2, No. 1, January 2013*. **2** (2013) 68–75.

[6] S. Priya Velammal, T.A. Devi, T.P. Amaladhas, Antioxidant, antimicrobial and cytotoxic activities of silver and gold nanoparticles synthesized using Plumbago zeylanica bark, *J. Nanostructure Chem.* **6** (2016) 247–260. https://doi.org/10.1007/s40097-016-0198-x.

[7] N. Basavegowda, A. Idhayadhulla, Y.R. Lee, Phyto-synthesis of gold nanoparticles using fruit extract of Hovenia dulcis and their biological activities, *Ind. Crops Prod.* **52** (2014) 745–751. https://doi.org/10.1016/j.indcrop.2013.12.006.

[8] N. Muniyappan, M. Pandeeswaran, A. Amalraj, Green synthesis of gold nanoparticles using Curcuma pseudomontana isolated curcumin: Its characterization, antimicrobial, antioxidant and anti-inflammatory activities, *Environ. Chem. Ecotoxicol.* **3** (2021) 117–124. https://doi.org/10.1016/j.enceco.2021.01.002.

[9] R. Vijayan, S. Joseph, B. Mathew, Costus speciosus rhizome extract mediated synthesis of silver and gold nanoparticles and their biological and catalytic properties, *Inorg. Nano-Metal Chem.* (2019). https://doi.org/10.1080/24701556.2019.1661439.

[10] B. Babu, S. Palanisamy, M. Vinosha, R. Anjali, P. Kumar, B. Pandi, M. Tabarsa, S.G. You, N.M. Prabhu, Bioengineered gold nanoparticles from marine seaweed Acanthophora spicifera for pharmaceutical uses: antioxidant, antibacterial, and anticancer activities, *Bioprocess Biosyst. Eng.* (2020). https://doi.org/10.1007/s00449-020-02408-3.

[11] X. Shi, C. Xue, F. Yu, T. Chen, H. Zhu, H. Xin, X. Wang, Functional Nanomaterials Engineered by Microorganisms, *Manuf. Nanostructures*. **13** (2014) 358–380.

[12] H. Shabestarian, M. Homayouni-Tabrizi, M. Soltani, F. Namvar, S. Azizi, R. Mohamad, H. Shabestarian, Green synthesis of gold nanoparticles using sumac aqueous extract and their antioxidant activity, *Mater. Res.* **20** (2017) 264–270. https://doi.org/10.1590/1980-5373-MR-2015-0694.

[13] A. Chahardoli, N. Karimi, F. Sadeghi, A. Fattahi, Green approach for synthesis of gold nanoparticles from Nigella arvensis leaf extract and evaluation of their antibacterial, antioxidant, cytotoxicity and catalytic activities, *Artif. Cells, Nanomedicine Biotechnol.* **46** (2018) 579–588. https://doi.org/10.1080/21691401.2017.1332634.

[14] M. Hamelian, S. Hemmati, K. Varmira, H. Veisi, Green synthesis, antibacterial, antioxidant and cytotoxic effect of gold nanoparticles using Pistacia Atlantica extract, *J. Taiwan Inst. Chem. Eng.* **93** (2018) 21–30. https://doi.org/10.1016/j.jtice.2018.07.018.

[15] M. Shahriari, S. Hemmati, A. Zangeneh, M.M. Zangeneh, Biosynthesis of gold nanoparticles using Allium noeanum Reut. ex Regel leaves aqueous extract; characterization and analysis of their cytotoxicity, antioxidant, and antibacterial properties, *Appl. Organomet. Chem.* **33** (2019) 1–11. https://doi.org/10.1002/aoc.5189.

[16] J.S. Boruah, C. Devi, U. Hazarika, P.V. Bhaskar Reddy, D. Chowdhury, M. Barthakur, P. Kalita, Green synthesis of gold nanoparticles using an antiepileptic plant extract:in vitrobiological and photo-catalytic activities, *RSC Adv.* **11** (2021) 28029–28041. https://doi.org/10.1039/d1ra02669k.

[17] Y. Hu, Y. Song, Y. Wang, J. Di, Electrochemical synthesis of gold nanoparticles onto indium tin oxide glass and application in biosensors, *Thin Solid Films*. **519** (2011) 6605–6609. https://doi.org/10.1016/j.tsf.2011.04.211.

[18] M. Etesami, F.S. Karoonian, N. Mohamed, Electrochemical deposition of gold nanoparticles on pencil graphite by fast scan cyclic voltammetry, *J. Chinese Chem. Soc.* **58** (2011) 688–693. https://doi.org/10.1002/jccs.201190107.

[19] B.A. Suliasih, D.G. Kurniawan, A. Auliya, M. Angelina, Scan rate Dependent Factor for Antioxidant Activity of Gold Nanofilms Synthesized via Cyclic Voltammetry Technique, *Chem. Mater.* **2** (2023) 51–55. https://doi.org/10.56425/cma.v2i2.60.

[20] I. Saldan, O. Dobrovetska, L. Sus, O. Makota, O. Pereviznyk, O. Kuntyi, O. Reshetnyak, Electrochemical synthesis and properties of gold nanomaterials, *J. Solid State Electrochem.* **22** (2018) 637–656. https://doi.org/10.1007/s10008-017-3835-5.

[21] S. Hosseingholilou, D. Dorranian, M. Ghoranneviss, Characterization of gold nanoparticle thin film prepared by electrophoretic deposition method, *Gold Bull.* **53** (2020) 1–10. https://doi.org/10.1007/s13404-020-00268-z.

[22] U.S. Mohanty, Electrodeposition: A versatile and inexpensive tool for the synthesis of nanoparticles, nanorods, nanowires, and nanoclusters of metals, *J. Appl. Electrochem.* **41** (2011) 257–270. https://doi.org/10.1007/s10800-010-0234-3.

[23] N.T. Nguyet, C. Van Tuan, D.T.T. Ngan, P.D. Tam, V.D. Nguyen, N.T. Nghia, Electrodeposited Fabrication of CeO2 Branched-like Nanostructure Used for Nonenzymatic Glucose Biosensor, *Crystals*. **13** (2023). https://doi.org/10.3390/cryst13091315.

[24] M. Etesami, N. Mohamed, Catalytic application of gold nanoparticles electrodeposited by fast scan cyclic voltammetry to glycerol electrooxidation in alkaline electrolyte, *Int. J. Electrochem. Sci.* **6** (2011) 4676–4689.

[25] R.A. Zayadi, F.A. Bakar, Comparative study on stability, antioxidant and catalytic activities of bio-stabilized colloidal gold nanoparticles using microalgae and cyanobacteria, *J. Environ. Chem. Eng.* (2020). https://doi.org/10.1016/j.jece.2020.103843.

[26] E. Musfiroh, Uji Aktivitas Peredaman Radikal Bebas Nanopartikel Emas dengan Berbagai Konsentrasi Sebagai Material Antiaging dalam Kosmetik, *UNESA J. Chem.* **1** (2012) 18–25.

[27] Y. Wang, S. Liu, M. Yang, A.A. Taha, J. Wang, C. Ma, Interaction effects on a gold nanoparticle-based colorimetric assay for antioxidant capacity evaluation of polyphenols, *RSC Adv.* (2020). https://doi.org/10.1039/d0ra01861a.

[28] R. Shunmugam, S. Renukadevi Balusamy, V. Kumar, S. Menon, T. Lakshmi, H. Perumalsamy, Biosynthesis of gold nanoparticles using marine microbe (Vibrio alginolyticus) and its anticancer and antioxidant analysis, *J. King Saud Univ. - Sci.* (2021). https://doi.org/10.1016/j.jksus.2020.101260.